A Panoramic Shortwave Infrared Hyperspectral Sensor for Maritime Sensing

K.P. Judd,[1] J.M. Nichols,[1] J. Waterman,[1] C.C. Olson,[2] K. Lee,[3] and G. Scriven[4]
[1]*Optical Sciences Division*
[2]*Sotera Defense Solutions, Inc.*
[3]*Thomas Jefferson High School for Science and Technology*
[4]*Opto-Knowledge Systems, Inc.*

Introduction: The U.S. Navy is exploring new technologies aimed at improving maritime electro-optic and infrared imaging systems. Specific goals include the enhancement of day/night, wide-area situational awareness; improved detection, identification, and tracking capabilities; and increased system reliability. Developing an imaging system that can accomplish these objectives is a tremendous design challenge, made even more difficult by the size, weight, and power limitations imposed on many shipboard and submarine imagers. In response to this challenge, the NRL Optical Sciences Division is leading the development of several compact, day/night imaging systems with resolution that supports detection and tracking of multiple contacts over a wide (360°) field of regard. The sensor system described here is one such example, driven by the Navy's Affordable Modular Panoramic Photonics Mast (AMPPM) program. The AMPPM program is aimed at creating several prototype imagers to serve as upgrades to the current *Virginia*-class submarine photonics masts.

Sensor System: In support of the AMPPM effort, the Maritime Sensing Section of the Applied Optics Branch, in collaboration with industry partners Brandywine Photonics and Smart Logic Inc., has developed a prototype hyperspectral shortwave infrared (SWIR) sensor for periscope applications. Current maritime imagers detect either the broadband emissive or reflective characteristics of an object; the resulting image data is then typically processed using either a point, blob (template matching), or more complex shape matching technique to automatically track the target. However, the image may not contain sufficient information to discriminate between true objects of interest and water- and land-based environmental clutter. The use of spectral imaging opens up the possibility of exploiting the unique optical characteristics that an object possesses to improve detection, identification, and tracking performance.[1] The shortwave infrared band, here defined as 0.9 to 1.7 micron, was selected as it has superior transmission characteristics through marine haze compared to the visible waveband and produces an image of comparable quality relative to visible sensor systems.

Ultimately, the limitation on physical space afforded a periscope imager dictates an aggressive optical design. This prototype therefore consists of a compact optical design Dyson spectrometer, a commercial 12-bit 640 × 512 InGaAs detector sensitive to radiation in the 0.9 to 1.7 micron waveband with thermoelectric cooling, and a commercial color-corrected 50 mm F/1.4 telescope (Fig. 1). The spatial data are aligned with the 640 pixel direction and the system has an instantaneous field of view (IFOV) of 0.5 mrad. The spectral resolution is ~8.7 nm with 111 bands illuminated. The sensor package is mounted to a variable speed pan/tilt unit that provides the scanning to generate the hyperspectral cube. Image acquisition, scanning, and real-time display of the data are computer controlled through a common graphical user interface (GUI). The scan speed and scan angle through which the sensor rotates determine the image width and final hyperspectral cube size.

Field Data and Processing: To examine the imaging quality, characteristics, and capabilities of the system, data were acquired of commercial and naval ship traffic through the port of San Diego from an elevated vantage point located at the tip of Point Loma in June 2012. During this time of year, a heavy marine layer persists until about mid-morning, producing challenging imaging conditions as can been seen in the visible quasi-stitched panoramic scene in the upper portion of Fig. 2. A typical maritime scene as represented by the false-color image of the hyperspectral data cube is shown at the bottom of the same figure. The bands chosen for the image are nominally the centers of the three major atmospheric transmission bandpass regions of the solar irradiance curve at sea level for the 0.9 to 1.7 micron waveband. A slow scan rate was used to create the high-fidelity image; however, slow scan rates translate into long scan periods and oversampling, which is not desirable for rapid object identification. Efforts are currently under way to minimize scan period while maximizing spatial and spectral content.

The processing effort is focused on determining the most efficient methods for classifying objects in the scene in real time so as to provide the operator with the most up-to-date information for rendering critical decisions. We have examined several such approaches, including creating spectral libraries for the maritime environment, applying matched filters to select spectral bands, creating models of relevant spectra using singular value decomposition (SVD) methods, and using more advanced techniques that leverage kernel principal component analysis (KPCA). Results of some recent studies are summarized in Fig. 3 using a standard receiver operating characteristic (ROC) curve. Current investigations are focused on incorporating

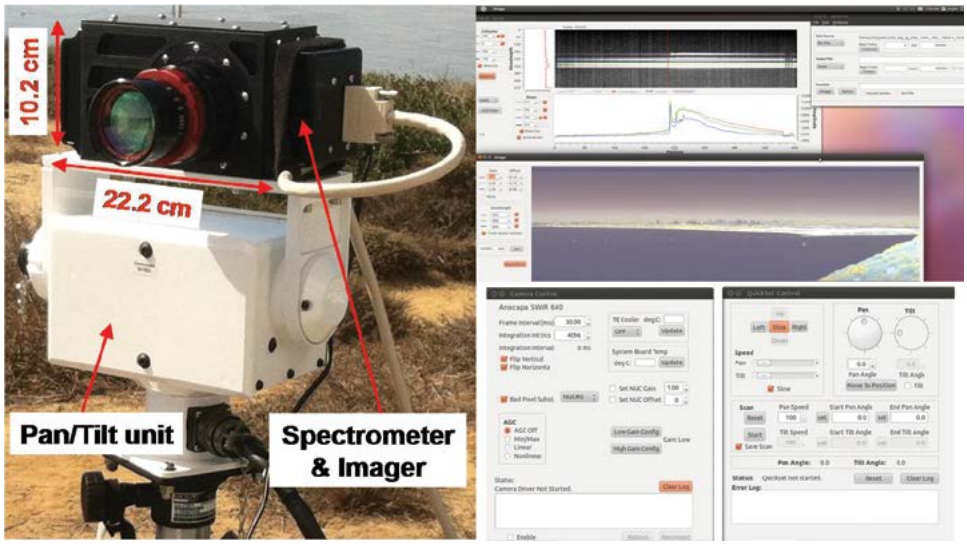

FIGURE 1
On the left is the sensor (black enclosure) mounted to the pan/tilt drive (white). At top right is the spectral signature map for selected wavelengths and corresponding real-time image displayed by the GUI; below are the camera interface and pan/tilt control windows.

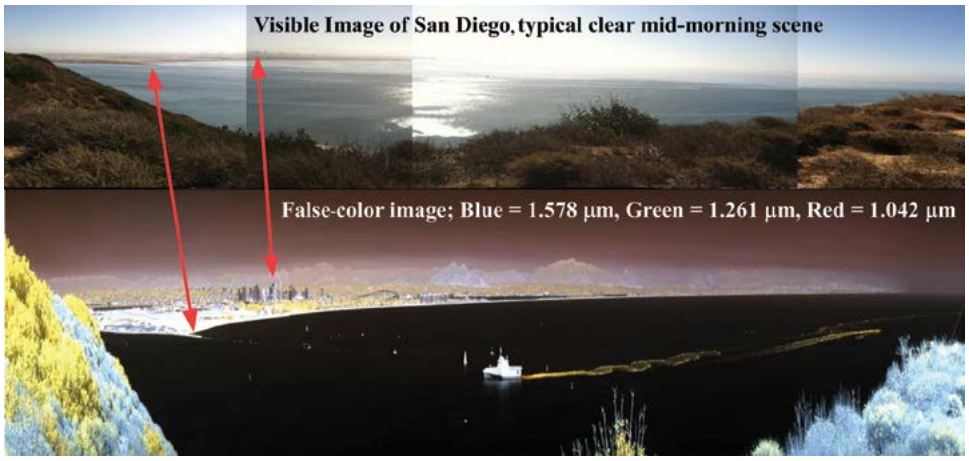

FIGURE 2
The top image is a quasi-stitched visible image of the entrance to San Diego harbor as seen from Point Loma. Below is a typical false-color image generated by the sensor using the wavelengths labeled on the image to display the hyperspectral data. The red arrows point to common locations in both representations of the scene, a breakwater on the left and downtown San Diego on the right.

locally measured meteorological parameters into the algorithms to improve detection performance.

Summary: We have developed and field tested a compact SWIR hyperspectral sensor for maritime applications. Current efforts are directed at reducing the dimensionality of the data and determining the most efficient machine learning algorithm for rapidly classifying objects of interest within the marine environment while maintaining good classification performance. This prototype is providing experience and laying the ground work for the future development of more advanced imaging systems.

Acknowledgments: We thank Dr. Costa Colbert of Smart Logic, Inc. and Dr. Dan Guerin of Brandywine Photonics for providing assistance during the field deployment.

[Sponsored by ONR]

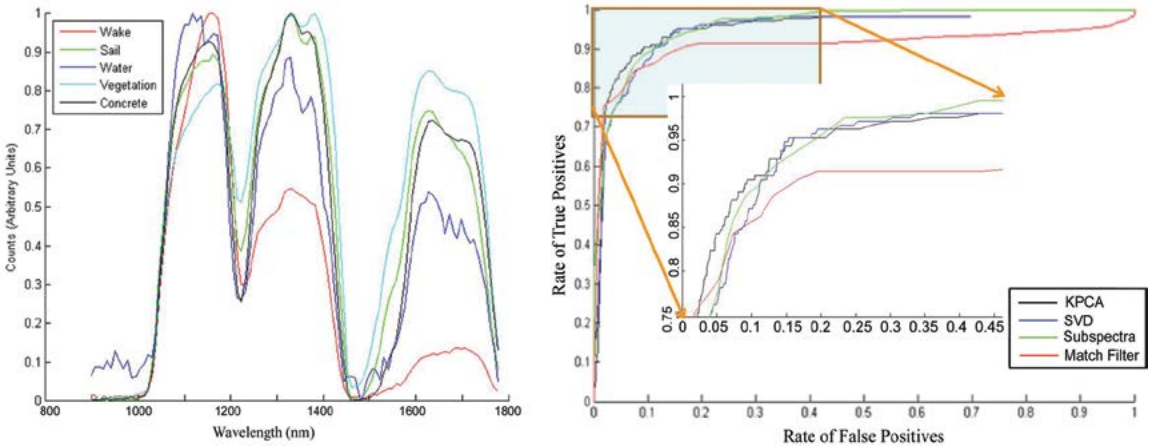

FIGURE 3
In the left panel are typical spectra of various objects of interest and clutter encountered in maritime environments. The right panel is an ROC curve for comparing the performance of several of the classification techniques. The inset is a magnification of the knee in the curve.

Reference
[1] K.P. Judd, J.M. Nichols, J.G. Howard, J.R. Waterman, and K.M. Vilardebo, "Passive Shortwave Infrared Broadband and Hyperspectral Imaging in a Maritime Environment," *Optical Engineering* **51**(1), 013202 (2012).

♦

Spatiotemporal-Multiplexed Quantum Dot Biosensors

M.H. Stewart,[1] W.R. Algar,[2] N. Hildebrandt,[3]
A. Huston,[1] and I. Medintz[4]
[1]*Optical Sciences Division*
[2]*University of British Columbia*
[3]*Université Paris-Sud*
[4]*Center for Bio/Molecular Science and Engineering*

Introduction: Colloidal nanocrystalline semiconductor quantum dots (QDs) possess unique size-tunable electronic and photophysical properties that can be exploited for a variety of Department of Defense (DoD)-relevant technological applications, such as sensors for explosives and chem/bio threats, theranostics (therapeutics and diagnostics), taggants, and photovoltaics. All of these applications rely on the controlled transfer of energy between QDs and selected energy donors and energy acceptors via fluorescence resonance energy transfer (FRET) and/or charge transfer (CT).[1] QD-based sensors that consist of a central QD, surrounded by dye-labeled bioreceptors, can be designed to respond to specific analytes that produce changes in the FRET rate, and therefore, the relative fluorescence intensities of the QD donors and the proximal dye acceptors. We recently demonstrated a nanoconstruct in which a single QD acts as a FRET intermediary, where the QD functions as both acceptor and donor in a FRET relay.[2] We further show that such QD platforms allow spectral and temporal multiplexing (i.e., simultaneous detection of multiple analytes) utilizing a single QD color, which has significant advantages over current state-of-the-art color-multiplexed QD platforms.

QD FRET Relay Platforms: The QD FRET relay system is composed of three optical components, as seen in Fig. 4(a): (1) A long lifetime luminescent terbium(III) complex (Tb) that acts as a FRET donor ($FRET_1$) to a (2) 625 nm–emitting QD ground state acceptor, which subsequently transfers energy ($FRET_2$) to a terminal (3) fluorescent Alexa Fluor 647 (A647) acceptor dye. The absorbance and photoluminescence (PL) spectra of each platform component are shown in Fig. 4(b), illustrating the spectral overlap and potential for successive energy flow from higher energy (blue) to lower energy (red) directly and over a time-gated window.

The FRET relay system was fabricated using polyhistidine–peptide linkers, developed under a previous NRL Institute for Nanoscience project, to tether the A647 (PEP A) and Tb (PEP B) to the QD surface (Fig. 4(a)). Using a ratiometric mixing format, FRET relay platforms could be formulated to link specific numbers of Tb and A647 to the QDs to yield Tb_n–QD–$A647_m$ assemblies. These platforms were developed in a collaborative effort between the Center for Bio/Molecular Science and Engineering, the Optical Sciences Division, and The Scripps Research Institute.

Time-Gated FRET: Short pulsed laser excitation of the FRET-relay system produces a mixture of excited-state QDs (QD*s) and Tb (Tb*) complexes. The shorter-lived QD*s (~50 ns) transfer energy rapidly to

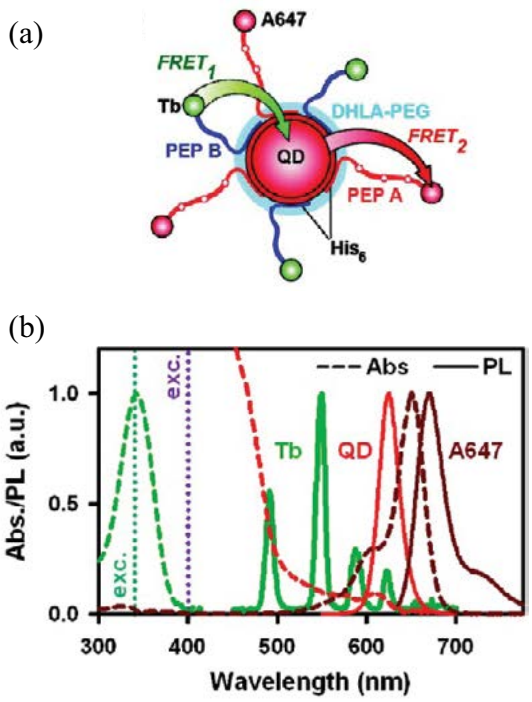

FIGURE 4
(a) QD serves as a nanoplatform for the assembly of A647- and Tb-labeled peptides, PEP A and PEP B, respectively. QD functions as an acceptor via Tb-to-QD $FRET_1$ and a donor via QD-to-A647 $FRET_2$. (b) Absorbance and emission spectra for Tb, QD, and A647. Figure adapted from Ref. 2.

the A647 dyes that, in turn, rapidly relax via the emission of light at ~670 nm. The long-lived Tb* complexes (2.6 ms) then transfer energy via $FRET_1$ to the relaxed QDs, over an extended period of time, which subsequently transfer energy to the A647 dyes via $FRET_2$ (Fig. 5). The QD acts as a time-stable energy conduit between the Tb complex and the A647 dye. Time-gating of the luminescence detection system allows one to utilize the immediate QD*-to-A647 FRET process independently from the time-delayed Tb*–QD–A647 FRET relay. The use of both the nongated and time-gated FRET provides two orthogonal FRET channels that can be used in a multiplexed format to detect two separate analytes within a single QD platform.

Two-plex DNA Hybridization Assay: To demonstrate this multiplexed format, a single QD platform was assembled to detect two separate nucleic acid hybridization events (Fig. 6(a)). QDs were conjugated with probe oligonucleotides, PRB A and PRB B, which capture the complementary target oligonucleotides TGT A–A647 and TGT B–Tb, respectively. The capture events were detected via nongated $FRET_2$ and time-gated $FRET_1$ and $FRET_2$ (Fig. 6(b)). The nongated ratio of A647/QD PL is proportional to the amount of hybridized TGT A–A647 and the time-gated sum of QD + A647 PL is proportional to the amount of hybridized TGT B–Tb per QD platform. This demonstrates that two orthogonal quantitative responses are detectable using a single QD platform.

Conclusions: NRL continues to develop powerful biosensors for DoD applications using energy transfer between QDs and peptide-linked donors and acceptors. We show that QDs can function as unique scaffolds and platforms to assemble FRET relays, where the QD behaves as both a FRET acceptor and donor in a time-gated format. Our work demonstrates that multiplexed sensing with a single QD color via spectrotemporal resolution of two orthogonal FRET processes is advantageous over current state-of-the-art QD multiplexing that relies on multiple QD colors. The time-gated FRET relay has been extended to multiplexed sensing of protease activity with a single QD vector, including the

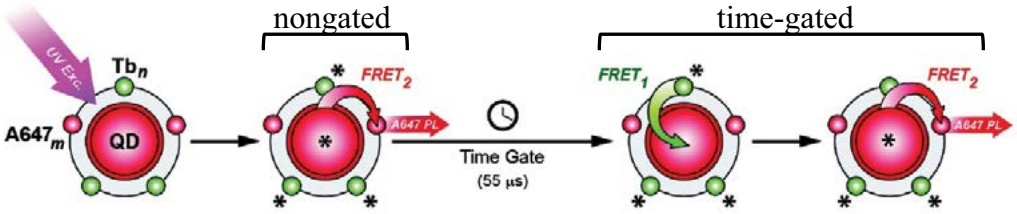

Time:	0 μs	< 250 ns	55 μs – 13 ms	55 μs – 13 ms
Tb:	ground state	excited state/good D	excited state/good D	excited state/good D
QD:	ground state	excited state/good D/poor A	ground state/good A	excited state/good D
A647:	ground state	ground state/good A	ground state/good A	ground state/good A
FRET:	–	$FRET_2$	$FRET_1$	$FRET_2$

FIGURE 5
Photophysical time-gated FRET relay process. Flash-excited QD*-to-A647 $FRET_2$ measured in nongated format. Excited state Tb* persists through microsecond delay (time gate). The ground state QD becomes a good FRET acceptor after a microsecond delay permitting the time-gated Tb*-to-QD $FRET_1$ and QD*-to-A647 $FRET_2$ energy cascade (D = donor, A = acceptor). Figure adapted from Ref. 2.

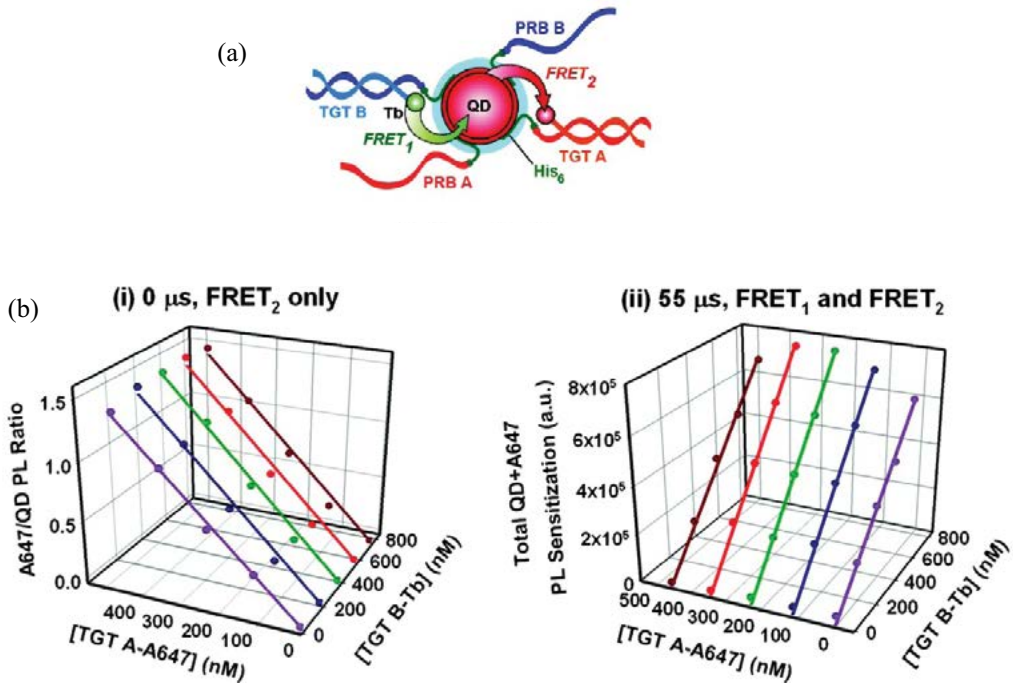

FIGURE 6
(a) Nucleic acid hybridization platforms. QDs conjugated with PRB A and PRB B engage in FRET upon capture of complementary TGT A–A647 and TGT B–Tb. (b) Orthogonal calibration curves for determining (i) TGT A–A647 hybridization via nongated $FRET_2$ data and (ii) TGT B–Tb via time-gated $FRET_1$ and $FRET_2$ data. Figure adapted from Ref. 2.

activation of an inactive pro-protease by another protease, which is a significant advancement in nanoparticle-based biosensing.[3]

Acknowledgments: The authors thank Lumiphore, Inc., for providing the Tb complex and Invitrogen by Life Technologies for the QDs.

[Sponsored by DTRA, DARPA, ONR, NRL Base Program (CNR funded), NRL Institute for Nanoscience, Innovative Medicines Initiative, and European Commission FP7]

References

[1] M.H. Stewart, A.L. Huston, A.M. Scott, A.L. Efros, J.S. Melinger, K.B. Gemmill, S.A. Trammell, J.B. Blanco-Canosa, P.E. Dawson, and I.L. Medintz, "Complex Förster Energy Transfer Interactions between Semiconductor Quantum Dots and a Redox-Active Osmium Assembly," *ACS Nano* **6**(6), 5330–5347 (2012).

[2] W.R. Algar, D. Wegner, A.L. Huston, J.B. Blanco-Canosa, M.H. Stewart, A. Armstrong, P.E. Dawson, N. Hildebrandt, and I.L. Medintz, "Quantum Dots as Simultaneous Acceptors and Donors in Time-Gated Förster Resonance Energy Transfer Relays: Characterization and Biosensing," *J. Am. Chem. Soc.* **134**(3), 1876–1891 (2012).

[3] W.R. Algar, A.P. Malanoski, K. Susumu, M.H. Stewart, N. Hildebrandt, and I.L. Medintz, "Multiplexed Tracking of Protease Activity Using a Single Color of Quantum Dot Vector and a Time-Gated Förster Resonance Energy Transfer Relay," *Anal. Chem.* **84**(22), 10136–10146 (2012).